Dalton Transactions

ROYAL SOCIETY OF CHEMISTRY

PAPER

View Article Online
View Journal | View Issue

Cite this: *Dalton Trans.*, 2025, **54**, 1689

Selective binding and fluorescence sensing of Zn(II)/Cd(II) using macrocyclic tetra-amines with different fluorophores: insights into the design of selective chemosensors for transition metals†

Giammarco Maria Romano, [a] Yschtar Tecla Simonini Steiner, [a] Francesco Bartoli,[b] Luca Conti, [a] Eleonora Macedi, [c] Carla Bazzicalupi, [a] Patrizia Rossi, [d] Paola Paoli, [d] Massimo Innocenti, [a] Andrea Bencini *[a] and Matteo Savastano [e]

Selective binding and optical sensing of Zn(II) and Cd(II) by L1, HL2, L3, H_2L4 and H_2L5 receptors were analysed in aqueous solutions by coupling potentiometric, UV-vis absorption and fluorescence emission measurements, with the aim to determine the effect of complex stability on selective signalling of metals with similar electronic configurations. All receptors share the same cyclic tetra-amine binding unit attached to a single quinoline (Q) or 8-hydroxyquinoline (8-OHQ) unit (L1 and HL2, respectively), two Q or 8-OHQ moieties (L3 and H_2L4, respectively), and, finally, two Q and two acetate groups (H_2L5). The crystal structures of the Cd(II) and Zn(II) complexes show that L3 and H_2L4 feature a cavity in which the larger Cd(II) complex is better fitted than the Zn(II) complex, leading to the formation of more stable Cd(II) complexes. In turn, Zn(II) forms more stable complexes with L1 and HL2, owing to its high tendency to give 5-coordinated complexes. Considering optical selectivity, Zn(II) gives the most emissive complex with L3, while the corresponding Cd(II) complex is basically quenched. The gathered structure of the Zn(II) complex, in which the two Q units are associated with one another—a structural motif not observed in the $[CdL3]^{2+}$ complex—leads to poor solvation of the Q units, favouring complex emission. Among 8-OHQ-containing receptors, the most emissive complex is formed by Cd(II) with HL2, containing a single 8-OHQ moiety. H_2L4 forms non-emissive complexes: the presence of two coordinating 8-OHQ moieties weakens metal interactions with the tetra-amine unit, favouring PET to the excited fluorophore that quench the emission.

Received 25th August 2024,
Accepted 10th December 2024

DOI: 10.1039/d4dt02415j

rsc.li/dalton

Introduction

Zinc and cadmium are two main transition metals that have been used in a variety of industrial processes, leading to their continuous spreading into the environment. Zinc is the second most abundant transition metal on Earth and is commonly used as an anti-corrosion agent, in most cases, *via* electrodeposition[1,2] of other metals or alloys, in particular iron and steel,[1] or as sacrificial anodes.[3] It is also used in several alloys, such as brass, bronze and nickel silver.[4] Besides industrial uses, zinc is an essential element for living organisms, as it is present in the active site of several enzymes that regulate cellular metabolism.[5] Furthermore, abnormal metabolism of Zn(II) ions, due to the consumption by or release from enzymes of 'free' Zn(II) in most cases, has been related to serious diseases, including ischemic stroke, prostate cancer and Alzheimer's disease.[6] Cadmium has been commonly used in industries such as Ni–Cd batteries, alloys, electroplating and solar cells.[7] Furthermore, today, long-term toxicity of cadmium and its compounds is well recognized. Exposure to this metal is known to cause serious diseases, ranging from cancer to disorders of the renal, gastrointestinal, neurological, reproductive, and respiratory systems.[7,8] As a matter of fact,

[a]*Department of Chemistry "Ugo Schiff", Università di Firenze, Via della Lastruccia 3, Sesto Fiorentino, Firenze, Italy. E-mail: andrea.bencini@unifi.it*
[b]*Dipartimento di Ricerca Traslazionale e delle Nuove Tecnologie in Medicina e Chirurgia, Via Savi 10, 56126 Pisa, Italy*
[c]*Department of Industrial Engineering, Università di Firenze, Via S. Marta 3, Firenze, Italy*
[d]*Department of Pure and Applied Sciences, University of Urbino "Carlo Bo", Via della Stazione 4, 61029 Urbino, Italy*
[e]*Department of Human Sciences for the Promotion of Quality of Life, Università San Raffaele Roma, via di Val Cannuta 247, 00166 Roma, Italy*

†Electronic supplementary information (ESI) available. CCDC 2375275–2375281. For ESI and crystallographic data in CIF or other electronic format see DOI: https://doi.org/10.1039/d4dt02415j

the use of this metal has been strongly limited by the regulatory bodies of EU community, fixing the maximum levels for its presence in the environment.[9] Zn(II) and Cd(II) determination and monitoring can be performed using several known methods, such as plasma-mass, atomic absorption or emission spectrometries. Fluorescence emission methods can alternatively be used, exploiting their ability to couple high sensitivity and performances with rapid, time-saving and cost-saving procedures.[10] The most common strategy to develop fluorescent chemosensors for metal cations couples within the same optical probe a binding unit, able to host the metal, forming stable complexes in solutions, and a fluorescent sensing moiety, in most cases, a heteroaromatic fluorophore, linked by a simple spacer, such as a short aliphatic chain. Binding of the metal induces changes in the emission properties and results in an optical signal (enhancement or decrease in the emission intensity and/or shift of the original band of the fluorophore).[11–15] Poor solubility in pure water and low selectivity in metal ion binding constitute the major drawbacks of this approach, particularly in the case of Zn(II) and Cd(II) complexation and signalling. In fact, the two metal cations have a d^{10} electron configuration and similar coordination features and often form complexes with comparable stability. Poor solubility in water can be overcome by using highly hydrophilic probes, while Zn(II)/Cd(II) selective binding can be achieved by designing probes containing coordination sites appropriately constructed to exploit the slight differences between the two metal cations such as the somewhat larger dimension of Cd(II) and/or its softer binding characteristics.[10] In most cases, the optical recognition of Cd(II) or Zn(II) has been related to the larger stability of the corresponding complexes. However, besides thermodynamic stability, other factors can influence the emission intensity, including electron, energy and proton transfer processes and conformational changes, which can be tuned by complexation.[11–16] Nevertheless, Zn(II)/Cd(II) optical discrimination is still a challenge. While fluorescent molecular optical sensors for Zn(II) are known from the 90s,[17] fluorescent probes able to discriminate Cd(II) from Zn(II) in water are less common.[18] Examples can be β-cyclodextrin-based receptors equipped with quinoline,[19] dansyl-containing polypeptides,[20] a perylene derivative conjugated with lactose and a dipicolylamine (DPA) binding unit,[21] a porphyrin fluorophore linked to DPA.[22]

In a recent paper we have reported on the synthesis and acid-base properties of receptors L1–L3 and H_2L5, analyzing the effect of receptor protonation on fluorescence emission. It was shown that the well-known emission of quinoline (Q) and 8-hydroxyquinoline (8-OHQ) are tuned by the presence of the tetra-amine macrocyclic unit (1,4,8,11-tetraazacyclododecane, cyclen) *via* the formation of hydrogen bonding or proton and electron transfer processes between the polyamine moiety and the fluorogenic units.[23] In this paper, we focused our attention on the effect of metal complexation with L1, HL2, L3 and H_2L5, extending our study to receptor H_2L4, which contains 2 8-OHQ units (Scheme 1). Cyclen has been often used as a binding unit for various transition metal cations. In particular,

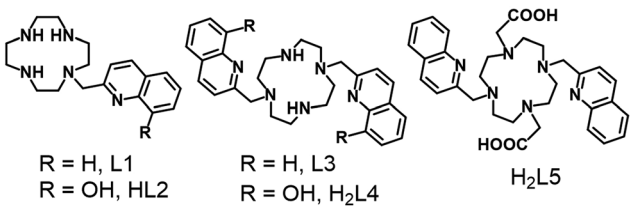

Scheme 1 Ligand drawings.

it can form stable complexes with the smaller first-row transition metals, including Zn(II).[17]

In these complexes, the metal is placed slightly above the mean plane of the four amine groups and normally completes its coordination sphere *via* coordination of a fifth donor atom from an exogenous ligand[21] or from a functional moiety linked to the macrocyclic structure.[24,25] The larger dimensions make the Cd(II) ion less suitable to fit the macrocyclic cavity of cyclen, and it generally lies more than 0.7 Å above the cyclen mean plane, completing its coordination environment *via* binding of a couple of external donors.[26]

The use of fluorescent pendant arms has been exploited to develop chemical sensors for Zn(II)[25] and, to a lesser extent, for Cd(II)[27] detection in water and/or biological media. Similarly, both Q and 8-OHQ are commonly employed as fluorescent signalling moieties for metal sensing including Zn(II) and Cd(II) detection.[11–16] Conversely, Q and 8-OHQ differ in their metal binding ability. While Q has a poor tendency to form stable complexes with transition metals, due to the low σ-donor ability of its nitrogen atom, 8-OHQ possesses an additional hydroxyl group, nicely placed to act, together with the heteroaromatic nitrogen, as a bidentate site for transition metals.[28] For instance, while Q forms poorly stable complexes with Zn(II) ($\log K < 2$) in water,[28] 8-OHQ, in its anionic form, gives stable 1 : 1 and 1 : 2 complexes with the same metal ($\log K_1 = 8.1$, $\log K_2 = 8.0$).[28,29] At the same time, metal coordination might inhibit the excited-state proton transfer from the hydroxyl group to the nitrogen atom of quinoline, a process that normally quenches the emission of 8-OH-Q.

Overall, the use of two signalling units with a similar structure, but remarkable different binding abilities, may allow for the analysis of the effect of thermodynamic stability of complexes on the ability of polyamine receptors to selectively signal similar metals, such as Zn(II) and Cd(II), in an aqueous solution, which is the main purpose of this paper.

Results and discussion

Proton binding in aqueous solutions

The analysis of the metal coordination properties of ligands L1–H_2L5 was performed by coupling potentiometric, spectrophotometric and spectrofluorimetric titrations in aqueous solutions. The process of ligand protonation, which competes with complex formation by polyamine ligands, has been previously reported for all receptors,[23] with the only exception of

the newly synthesized H_2L4. However, the protonation properties of the latter parallel those found for HL2, for which the formation of a deprotonated species, $L2^-$, was observed at strongly alkaline pH values, whose protonation originates the HL2 species in a zwitterionic form.[23] Potentiometric titrations performed on H_2L4 allow for the determination of the protonation equilibria occurring in solutions and the corresponding equilibrium constants, reported, together with those of ligand HL2, in Table 1 (the distribution diagram of the protonated species of H_2L4 are given in Fig. S6,† while the protonation constants of all receptors studied are shown in Table S1, see ESI†).

Similar to HL2, in the case of H_2L4, an anionic species ($L4^{2-}$) is formed at alkaline pH values. This species can bind up to five H^+ ions in aqueous solutions. At strongly alkaline pH values (pH > 10, Fig. S7†), the UV-vis absorption spectra feature a broad band at *ca.* 340 nm, attributable to the presence of deprotonated 8-OHQ moieties in the $L4^{2-}$ and $HL4^-$ species. Upon decreasing the pH, this band tends to disappear and a new band at 300 nm appears in the spectra with the formation of species at a higher protonation degree, in which the hydroxyl group of 8-OHQ is protonated, as already found in HL2.[23]

The superimposition of the absorbance values at 300 and 340 nm with the distribution diagram of the protonated species (Fig. S8†) points out that the appearance of the 300 nm band below pH 10 accompanies the formation of the H_4L4^{2+} species in solutions. The latter would contain both hydroxyl groups in their protonated neutral form and two protonated amine groups of the macrocyclic moiety, while the species with a lower protonation degree would feature one or both deprotonated 8-OHQ moieties. This hypothesis is basically confirmed by the analysis of the pH dependence of the fluorescence emission spectra (Fig. S9†). At acidic pH values, the spectra feature a band at 410 nm, which is attributed to the neutral (non-zwitterionic) 8-OHQ fluorophore. By increasing the pH, the typical band at 525 nm of deprotonated 8-OHQ[23] appears in the spectra recorded at alkaline pH values. This spectral change occurs upon the deprotonation of the H_4L4^{2+} species to give the less protonated forms H_3L3^+, H_2L3 and $HL3^-$ (Fig. S10†), in which the receptor is in zwitterionic form, with at least one acidic proton being bound by the amine groups of the receptor.

Table 1 Protonation constants of HL2 and H_2L4 (298 K, 0.1 M NMe_4Cl (HL1) or 0.1 M NaCl (H_2L2))

Equilibrium	Log K^a	Equilibrium	Log K
$L2^- + H^+ = [HL2]$	11.06(6)	$L4^{2-} + H^+ = [HL4]^-$	11.01(4)
$[HL2] + H^+ = [H_2L2]^+$	10.54(5)	$[HL4]^- + H^+ = [H_2L4]$	10.66(7)
$[H_2L2]^+ + H^+ = [H_3L2]^{2+}$	8.85(5)	$[H_2L4] + H^+ = [H_3L4]^+$	9.90(6)
$[H_3L2]^{2+} + H^+ = [H_4L1]^{3+}$	2.88(7)	$[H_3L4]^+ + H^+ = [H_4L4]^{2+}$	9.2(1)
		$[H_4L4]^{2+} + H^+ = [H_5L4]^{3+}$	3.9(1)

[a] Values taken from ref. 23.

Crystal structures of the complexes

The slow evaporation of aqueous solutions containing a single receptor and a metal in 1/1 molar ratio at neutral pH in the presence of an excess of $NaClO_4$ leads to the formation of crystals, suitable for single-crystal X-ray diffraction (SCXRD), of the metal complexes as perchlorate salts. This approach failed in the case of H_2L5. As an attempt to obtain crystals suitable for SCXRD analysis, we also added $MgCl_2$ or $CaCl_2$ to the solutions (both Mg(II) and Ca(II) are strongly bound by carboxylate groups, but form less stable complexes with polyamine–polycarboxylate ligands than the metals under investigation). This leads to the crystallization of the mixed complex $[Ca(ZnL5)_2](ClO_4)_2{\cdot}14H_2O$.

$[CuL1](ClO_4)_2{\cdot}0.5H_2O$. The Cu(II) complex with the monoquinoline ligand L1 copper complex crystallized as the monohydrate perchlorate salt of its Cu(II) complex: $[CuL1](ClO_4)_2{\cdot}0.5H_2O$. A view of the $[CuL1]^{2+}$ cation is presented in Fig. 1, together with that, previously reported,[30] of the $[ZnL1]^{2+}$ cation.

Similarly to $[ZnL1]^{2+}$ (see Fig. 1 and Fig. S11† for comparison), the complex can be described as a distorted square pyramid (τ_5 = 0.073),[32] whose square base is constituted by the 4 macrocyclic N donors, while the quinoline nitrogen occupies the apical position. The metal cation rests almost coplanar with the 4 macrocyclic donors, protruding from their median plane by only 0.531(2) Å. In $[ZnL1]^{2+}$, the metal is slightly more displaced from the square-based plane (0.725(5) Å). The Zn–N distances range from 2.019 to 2.166 Å (mean distance 2.10(3) Å). The macrocycle overall conformation can still be regarded as a [3333]C corner conformation.[31] Despite the poor binding of the Q nitrogen with respect to aliphatic amine groups, the Zn–N5 distance is comparable to those between the metal and the cyclen amine groups. Furthermore, the short methylene linker between the tertiary amine N3 and the Q pendant arm allows N5 to assume a position close to the metal, with the formation of a stabilizing 5-term chelating ring. Among the $[ZnL1]^{2+}$ and $[CuL1]^{2+}$ cations, in the Cu(II) complex, the axial Q nitrogen is furthest from the metal centre, easily justified in a Jahn–Teller framework.

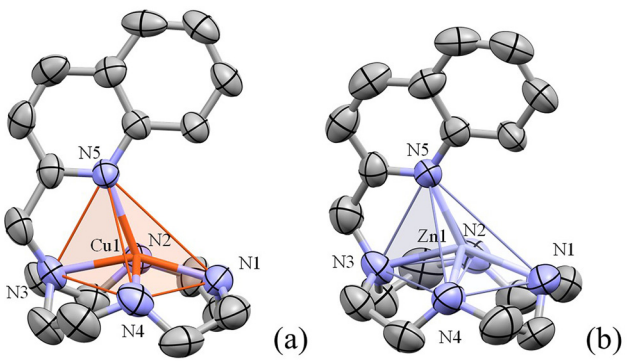

Fig. 1 Coordination geometry and labelling scheme for the $[CuL1]^{2+}$ (a) and $[ZnL1]^{2+}$ (b) complexes (ORTEP drawing at 50% probability; H atoms omitted for clarity).

Full metrics, distances and angles, are given in Table S2.†

$[ZnL3](ClO_4)_2\cdot 0.5H_2O$ and $[CdL3](ClO_4)_2\cdot H_2O$. The obtained solid-state complexes of the bisquinoline derivative L3 present similar formulas, $[ZnL3](ClO_4)_2\cdot 0.5H_2O$ and $[CdL3](ClO_4)_2\cdot H_2O$, and virtually identical coordination modes; the size difference among the two metal cations results in different π–π stacking possibilities of the fluorophores.

Both metals achieve hexa-coordination exploiting all N donors present in the ligand; the overall coordination geometry can be described as a slightly distorted trigonal prism for both cases (Fig. 2), with the trigonal faces each defined by two vicinal nitrogen donors of the macrocycle and a quinoline one. Full coordination metrics are given in Table S3.†

Both macrocycles are found in the usual [3333]C corner conformation. The metal cation is slightly above the mean plane defined by the four macrocycle nitrogen atoms (0.908(2) and 1.158(1) Å for Zn(II) and Cd(II), respectively), with the N quinoline donors completing hexa-coordination, both lying on the same side with respect to the macrocycle. The Zn–N bond lengths are in the range of 2.160–2.227 (Table S3†) (mean distance 2.20(3) Å), while the Cd–N one ranges between 2.337 and 2.405 Å (mean 2.36(2) Å).

The main difference among the two similar complexes lies in the mutual disposition of the quinoline pendants, which is dictated by the size difference among the cations, as it can be appreciated from Fig. 3.

Bulkier Cd(II), which also lies somewhat further from the macrocycle 4 nitrogen mean plane (*cf.* above), gives larger N5–M–N6 angles, 100.09(6)° *vs.* 86.6(1)° for Zn(II) (Table S3†), implying a more significant spreading apart from the quinoline pendants. In the case of the more gathered Zn(II) complex, the two aromatic moieties are able to maintain an angle of 29.7(2)° among their mean planes (centroid to centroid distance: 3.682(5) Å), engaging in π–π stacking contacts. On the contrary, the more open Cd(II) complex features a quinoline–quinoline mean plane angle of 51.22(5)°, which prevents π–π stacking. If such solid-state conformations are any close to solution ones, it can be expected that the Zn(II) complex, more gathered and able to better protect its fluorophore from the environment, should be found more emissive with respect to the Cd(II) one.

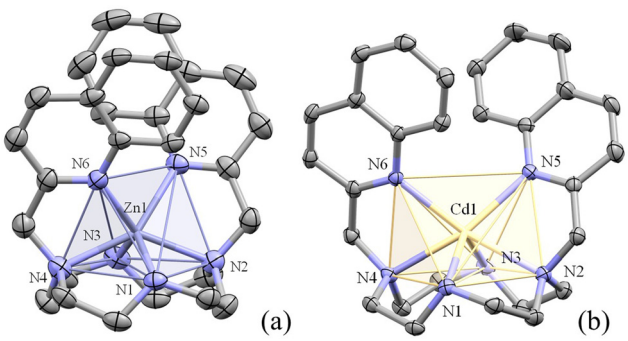

Fig. 2 Coordination geometry and labelling scheme for $[ZnL3]^{2+}$ (a) and $[CdL3]^{2+}$ (b) complexes, showing similar distorted trigonal prism coordination environments. Ellipsoids drawn at the 50% probability level. Hydrogen atoms are omitted for clarity.

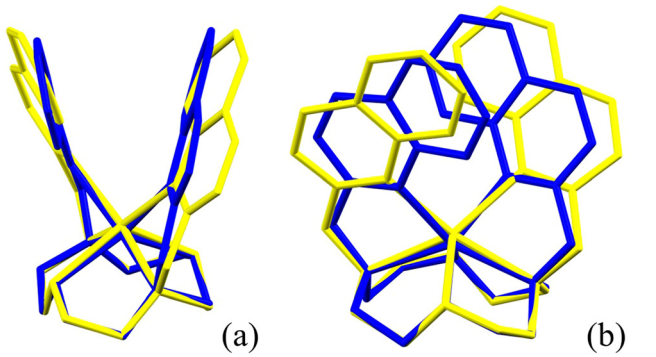

Fig. 3 Side (a) and lateral (b) views of the superposition of the Zn(II) (blue) and Cd(II) (yellow) complexes (4 macrocycle nitrogen atoms superimposed, RMS 0.0701 Å).

$[M(H_2L4)](ClO_4)_2\cdot H_2O$ (M = Zn or Cd) and $[Pb(HL4)]ClO_4\cdot 2H_2O$. The obtained solid complexes of the bis-hydroxyquinoline ligand present different formulas and coordination modes instead, mostly due to metal preferences in terms of coordination numbers, types of donors, and different engagements of the phenol/phenolate group in metal binding: this last aspect obviously affects complex charge and hence formulas of the solids, which are as follows: $[Zn(H_2L4)](ClO_4)_2\cdot H_2O$, $[Cd(H_2L4)](ClO_4)_2\cdot H_2O$, and $[Pb(HL4)]ClO_4\cdot 2H_2O$.

A synopsis of the three complexes is presented in Fig. 4, while Table S4† summarizes the coordination metrics for all complexes.

The Zn(II) complex is the only one of the series where hydroxyl groups are not involved in metal binding, N donors being both preferred and in sufficient number (6) to fully fulfil the metal stereoelectronic requirements. The metal coordination environment can be described starting from the $[ZnL3]^{2+}$ above example. The macrocycle maintains the [3333]C corner conformation, the coordination geometry remains a trigonal prism, with both triangular faces defined by two donors of the macrocycle and one quinoline nitrogen, the metal is found slightly above the mean macrocyclic N plane (0.944(4) Å *vs.* 0.908(2) Å for $[ZnL3]^{2+}$), and the overall arrangements are closely related, as can be appreciated by superimposing the structures (Fig. S12†). Moreover, in this case, among the three metal complexes featuring H_2L4, the Zn(II) complex presents the lowest angle in between hydroxyquinoline N donors (N5–Zn1–N6 88.2(3) Å, Table S4†), which results in a low angle among the average planes of the two fluorophore moieties (22.7(2)°). This, again, results in a number of stabilizing π–π stacking contacts among the fluorogenic units.

The heavier Cd(II) ion, given the abundance of donor atoms in the ligand and the good chelating ability of hydroxyquinoline, is instead observed to expand its coordination number to 8, adopting now a typical slightly distorted square antiprism geometry. The 4 nitrogen atoms of the macrocycle and the 4 (2 N and 2 O) donors of the hydroxyquinolines define the two

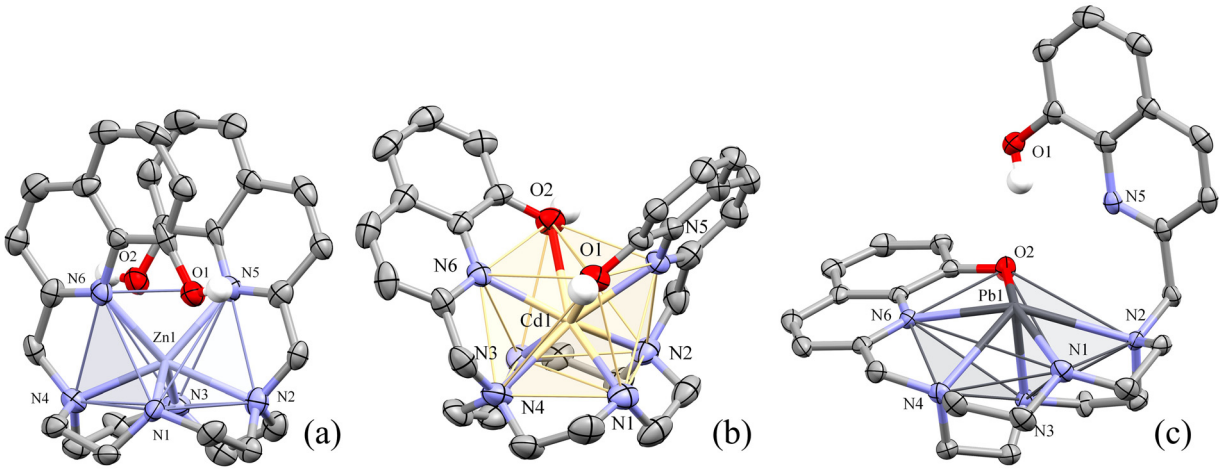

Fig. 4 Coordination geometry and labelling scheme for the $[Zn(H_2L4)](ClO_4)_2{\cdot}H_2O$ (a), $[Cd(H_2L4)](ClO_4)_2{\cdot}H_2O]$ (b) and $[Pb(HL4)]ClO_4(H_2O)_2$ (c) complexes, showing different coordination environments. Ellipsoids are drawn at the 50% probability level. Only hydroxyl hydrogens are explicitly shown to highlight differences in the protonation state of the ligand.

parallel square faces (average angle between the average planes of aforementioned groups of donor atoms 1.4(2)°). The Cd center is found closer to the macrocyclic N donors' average plane (1.276(4) Å) than to its hydroxyquinoline donor counterpart plane (1.493(3) Å), according to the fact that Cd–O distances are found significantly longer than the Cd–N distances (Table S4†). It should be noted that, in the Cd(II) case, the involvement of the hydroxyl group in metal binding does not trigger its deprotonation. However, this complex was obtained from crystallization in water solution at pH 7, where $[CdL(H_2L4)]^{2+}$ is the unique species detected in solution by potentiometric titrations. While the macrocycle retains the [3333]C corner conformation, the binding is significantly affected by oxygen coordination with respect to the [CdL3] complex, and the N5–Cd–N6 angle widens even more (116.2(2)° for $[CdL(H_2L4)]^{2+}$ and 100.09(6) for $[CdL3]^{2+}$, Tables S4 and S3,† respectively). This results in a further spreading apart of the hydroxyquinoline moieties, which now feature an angle of 85.5(2)° between their mean planes, totally preventing any π–π stacking contact.

The Pb(II) complex is perhaps the most diverse. The metal presents a distorted pentagonal pyramidal coordination environment, with the other side of the pentagonal plane entirely devoid of ligands: this coordination mode has been observed in multiple instances and is generally rationalized due to the presence of stereochemically active electronic doublet on the Pb(II) centre.[33] This peculiar arrangement leads to the deprotonation of one of the fluorophore hydroxyl groups. The other one remains protonated and O1···O2 intramolecular H bond 2.754(4) Å is formed (O1–H1O···O2 angle 152(5) and H1O···O2 distance 1.99(3) Å). Since hydroxyquinoline oxygen atoms lay in the respective aromatic plane, the presence of the hydrogen bond fosters an angle among the fluorophore planes of 75.40(8)° (obtuse angle 104.46(8)°, *i.e.*, close to tetrahedral, as required by the intramolecular H-bond). The only π–π stacking interactions present are thus intermolecular among non-coordinated hydroxyquinoline moieties (not coordinated quinoline plane···quinoline plane distance 3.526(4) Å).

$[Ca(ZnL5)_2](ClO_4)_2{\cdot}14H_2O$. The only isolated crystalline compound of the ligand H_2L5 is $[Ca(ZnL5)_2](ClO_4)_2{\cdot}14H_2O$ presenting a unique $[Ca(ZnL5)_2]^{2+}$ trinuclear complex (Fig. 5).

The Zn1A abd Zn1B metal cations are 6-coordinated. In both cases, the macrocycle adopts a distorted [2424]C corner conformation and two oxygen donors, each one belonging to a ligand carboxylate group, complete theoverall trigonal prismatic environment of the metal. One Zn-bound carboxylate per ligand also chelates the Ca(II) ion, whose binding site is

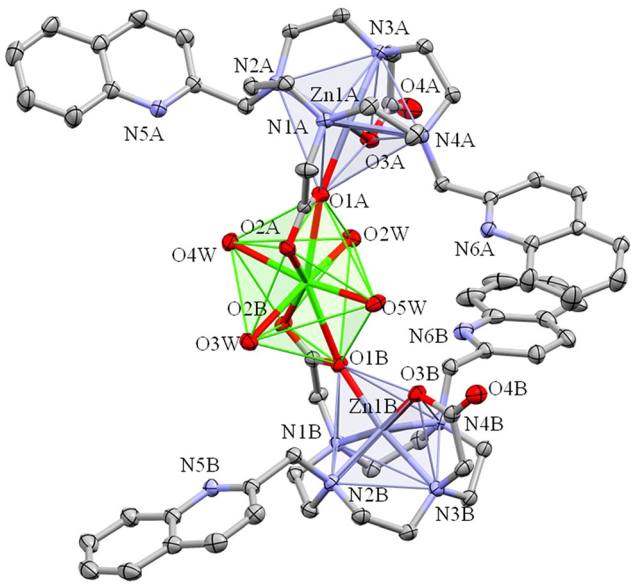

Fig. 5 Coordination geometry and labelling scheme for the $[Ca(ZnL5)_2]^{2+}$ trinuclear complex. Ellipsoids drawn at the 50% probability level. Hydrogen atoms are omitted for clarity.

therefore defined by the two Zn(II) complexes. Four water molecules complete the Ca(II) coordination environment, which can be described as a distorted dodecahedron. Full coordination metrics are reported in Table S5.†

The angle among the two Zn(II) centres defining the Ca(II) binding site (defined as the angle in between 2 N and 2 O donors of each macrocycle, namely N3B N1B O3B O1B and N1A N3A O1A O3A) is 72.23(5)°. The non-Ca(II)-chelating carboxylate of each ligand is involved in H-bond formation with first sphere Ca(II)-coordinating water molecules (Table S7†). The 4 quinoline N atoms of each ligand pair are all involved in solvent-bridged H-bonding to the Ca(II) first coordination sphere, thus offering further stabilization to the trinuclear complex. A view of the main hydrogen bonds stabilizing the trinuclear complex is presented in Fig. 6 (metrics in Table S6†).

Stability of the metal complexes in aqueous solutions

Considering metal binding in aqueous solutions, we focused our attention on four metal cations, namely, Zn(II), Cd(II), Pb(II) and Cu(II). Zn(II) and Cd(II) represent exemplifying cases of metals which often give with polyamine ligands emissive complexes, featuring similar stability in aqueous solution. Both stability and emission are tuned by ligand structural properties, such as the presence of different pendant arms linked to the tetra-amine macrocycle, as in the case of L1–H_2L5, which would control both their thermodynamic and sensing selectivity for Zn(II) over Cd(II) or *vice versa*. Cu(II) and Pb(II) were chosen, respectively, as examples of paramagnetic and heavy metals, which generally quench the emission of polyamine receptors. Table 2 reports the species formed by these metal cations and their stability constants, obtained by means of potentiometric titrations, while Fig. 7 displays the distribution diagrams for the complexes formed by Zn(II) and Cd(II)

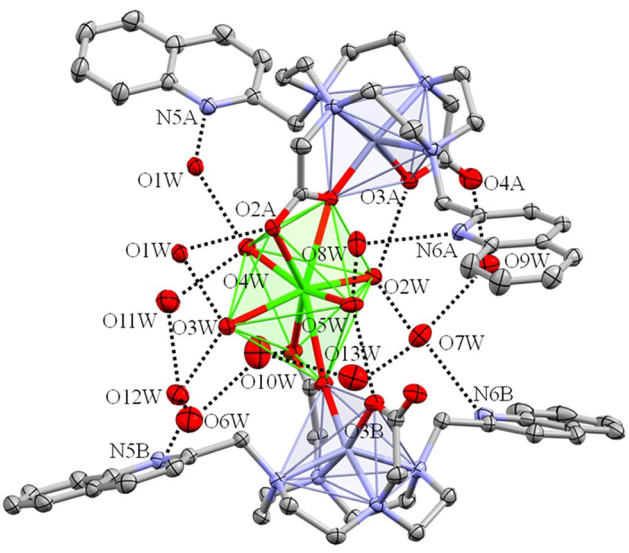

Fig. 6 Main intramolecular and solvent-bridged H-bonds stabilizing the $[Ca(ZnL5)_2]^{2+}$ trinuclear complex. Ellipsoids drawn at the 50% probability level. Hydrogen atoms are omitted for clarity.

Table 2 Formation constants of the complexes with L1, HL2, L3, H_2L4 and H_2L5 (298 K, 0.1 M NaCl)

Equilibrium	Cu(II)	Zn(II)	Cd(II)	Pb(II)
L = L1				
$M^{2+} + L = [ML]^{2+}$	19.5(1)	16.37(3)	15.17(2)	—
$[ML]^{2+} + H^+ = [MHL]^{3+}$	3.01(4)	3.77(3)	3.57(9)	—
$[ML]^{2+} + OH^- = [ML(OH)]^+$	—	2.27(6)	1.8(1)	—
L = L2				
$M^{2+} + L^- = [ML]^+$	—	18.76(6)	16.92(3)	16.6(1)
$M^{2+} + HL = [M(HL)]$	—	17.93(6)	16.02(3)	15.2(1)
$M^{2+} + (H_2L)^+ = [M(H_2L)]^{3+}$	—	10.85(6)	9.46(3)	8.87(9)
L = L3				
$M^{2+} + L^+ = [ML]^{2+}$	18.67(6)	16.24(1)	16.98(4)	—
$[ML]^{2+} + H^+ = [MLH]^{3+}$	2.4(1)	5.65(7)	3.58(5)	—
L = L4				
$M^{2+} + L^{2-} = [LM]$	21.30(4)	17.80(1)	18.70(1)	15.1(2)
$M^{2+} + [HL]^- = [M(HL)]^+$	21.17(5)	17.49(1)	18.39(1)	14.69(3)
$M^{2+} + H_2L = [M(H_2L)]^{2+}$	20.03(2)	17.03(1)	17.83(1)	13.33(2)
L = L5				
$M^{2+} + L^{2-} = [ML]$	23.6(1)	19.2(1)	20.5(1)	—

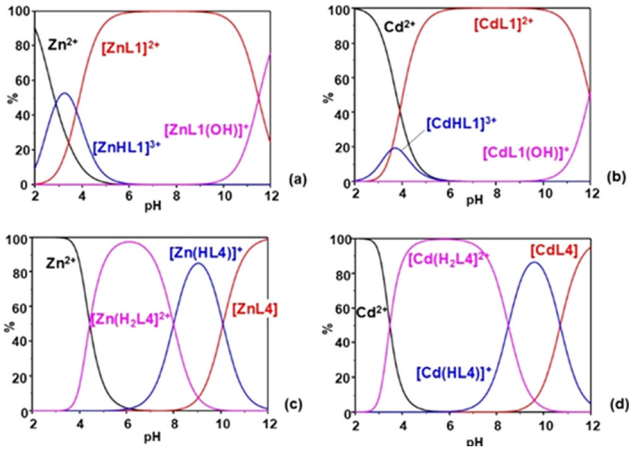

Fig. 7 Distribution diagrams formed by L1 with Zn(II) (a) and Cd(II) (b) and by H_2L4 with Zn(II) (c) and Cd(II) (d) (298 K, [L] = $[M^{2+}]$ = 0.001 M and 0.1 M NaCl).

with L1 and H_2L4 (the distribution diagrams for the other systems are given in the ESI; Fig. S13–S17†). In some cases (Cu(II) complexes with L1, all H_2L5 complexes), precipitation is observed at alkaline pH values (above pH 8), probably due to the formation of poorly soluble hydroxo-complexes, preventing the speciation study in the alkaline region. The Pb(II) complexes with L1, L3 and H_2L5 suffer low solubility in the whole pH range investigated (2.5–10.5), preventing any reliable speciation study.

The potentiometric titrations point out the formation of complexes with a metal-to-ligand stoichiometry of 1 : 1 for all ligands under investigation, ruling out the formation of complexes with higher nuclearity. Cu(II) forms the most stable complexes, due to the stabilizing effects of CFSE. The complexes of Zn(II), Cd(II) and Pb(II) with polyamine-based ligands often show similar stability in aqueous solutions. In the present case, receptors L1–H_2L4 show different binding abil-

ities toward Zn(II) and Cd(II), depending on the number of the heteroaromatic units linked to the macrocyclic moiety. In these complexes, heteroaromatic nitrogen is normally involved in metal coordination, as testified by the crystal structures reported above, with the only exception of the Pb(II) complex with H_2L4, in which only one heteroaromatic unit is involved in metal binding, probably due to the presence of a stereochemically active lone pair on the metal.[33] Both L1 and HL2, featuring a single hetero-aromatic unit, form more stable 1 : 1 complexes with a smaller Zn(II) ion than with Cd(II) and Pb(II). Furthermore, Zn(II) displays a high tendency to form stable penta-coordinated complexes, although it can expand its coordination sphere to achieve hexa-coordination, as actually observed in the crystal structure of $[ZnL3]^{2+}$ and $[Zn(H_2L4)]^{2+}$ complexes, while Cd(II) and Pb(II) preferentially form hexa-coordinated species and they can also achieve larger coordination numbers. This could justify the somewhat higher stability of the cadmium complexes with receptors L3, H_2L4 and H_2L5, which contain a larger number of nitrogen atoms and six or more potential donor atoms, with respect to the corresponding zinc complexes. The $[CdL3]^{2+}$, $[Cd(H_2L4)]^{2+}$ and [CdL5] complexes are *ca.* 5, 6 and 20 times more stable than the corresponding complexes with Zn(II), respectively.

From this point of view, the crystal structure of the $[ZnL1]^{2+}$ complex showed that the Zn(II) ion is firmly bound by the 5 nitrogen donors.[30] As normally observed in complexes of 1,4,7,10-tetraazacyclodecane, in $[ZnL1]^{2+}$, the metal lies above the mean plane defined by the 4 N donors of the macrocyclic ring (0.725(5) Å).[30] The Zn–N distances range between 2.019 and 2.166 Å (mean distance 2.10(3) Å), slightly lower than that found in Zn(II) complexes usually found with polyamine ligands (2.16(9) Å).[34] In the $[ZnL3]^{2+}$ cation, the metal is displaced 0.908(2) above the mean plane of the 4 aliphatic amine nitrogens and achieves hexa-coordination at the expense of the formation of somewhat longer Zn–N bond lengths, which are in the range of 2.160–2.227 (Table S3†), with a mean distance of 2.20(3) Å, somewhat longer than that observed for the $[ZnL1]^{2+}$ cation (2.10(3) Å). In the case of $[CdL3]^{2+}$, the metal is located 1.158(1) Å above the mean plane of aliphatic amines and the Cd–N distances span in the range 2.337–2.405 Å (mean 2.36(2) Å). These values are in the typical range observed in Cd(II) complexes with polyamines and would account for stronger metal–nitrogen interactions with respect to the $[ZnL3]^{2+}$ complex, which may contribute to justify the higher stability of the Cd(II) complex with L3 with respect to the L1 one.

In the case of Zn(II) and Cd(II) complexes with H_2L4, the metals are located 0.944(4) and 1.276(4) Å, respectively, above the plane defined by the 4 aliphatic amine groups. The coordination of Cd(II) with both nitrogen and hydroxyl groups of two 8-OHQ moieties implies the formation of somewhat weaker interactions with the macrocyclic amines, but allows Cd(II) to achieve octa-coordination, resulting in an overall complex stabilization. Conversely, in the corresponding Zn(II) complex, the Zn–N mean distance is 2.21(3) Å, indicating the formation of Zn–N contacts even weaker than that observed in the $[ZnL3]^{2+}$ cation, while no interaction occurs between the OH groups of 8-OHQ and the metal.

Although hypothesis on complex stability based on X-ray crystal structure data can sometimes lead to misleading conclusions, the panorama depicted by the Zn(II) and Cd(II) solid-state structures suggests that receptors containing two heteroaromatic subunits define a cleft dimensioned to optimally host the larger Cd(II) ion, which can easily form more stable complexes. Zn(II) still fits the ligand pocket, giving, however, slightly weaker interactions with the nitrogen donors than Cd(II).

Conversely, L1 and HL2, containing five nitrogen donors form more stable complexes with Zn(II) (the hydroxyl group of HL2 is probably not bound to the metal) with respect to Cd(II), probably due to the higher tendency of Zn(II) to form penta-coordinated complexes than Cd(II).

Comparing the binding ability of receptors containing Q or 8-OHQ (in its neutral form) moieties, HL2 and H_2L4 form respectively more stable complexes than L1 and L3 with all metals under investigation. For instance, the formation constants of the Zn(II) complexes with L1 and HL2 are 16.17 and 18.76 log units, respectively, while the formation constants of the L3 and H_2L4 complexes with the same metal are 16.24 and 17.03 log units, respectively. This result is in agreement with the presence of an 8-OHQ bidentate moiety, a better chelating agent for metal than simple Q, in HL2 and H_2L4.[28] At the same time, the hydroxyl electron-donor group can increase the electron density on the quinoline moiety, enhancing the donor ability of its heteroaromatic nitrogen. The only exception to this rule is the Q-containing receptor H_2L5, which gives more stable Zn(II) and Cd(II) complexes than all the other ligands. This reflects a higher binding ability of an acetate than a Q or 8-OHQ moiety,[28] as also testified by the crystal structure of the [ZnL5] complex, in which the metal is coordinated by the two acetate groups, while the two Q units are not bound to Zn(II). Noteworthy, no protonated forms of the complex were detected by potentiometric titrations in aqueous solutions at pH 7 or at an even lower pH value (Fig. S17†).

The presence of the Q or 8-OHQ group also influences the species formed by metals with different receptors. Potentiometric titrations show that the solution chemistry of L1 and L3 is featured by the formation of a stable $[ML]^{2+}$ species (L = L1 or L3), largely prevalent at a neutral pH value, as shown in Fig. 7a and b for the Zn(II) and Cd(II) complexes with L1 (see Fig. S13–S17† for the other complexes). The protonation of the complexes can occur at acidic pH values to give $[MLH]^{+}$ species. In the case of the 8-OHQ-containing receptors HL2 and H_2L4, the formation of deprotonated complexes of the type $[ML2]^{+}$ and $[M(HL4)]^{+}$ or [ML4] is not detected at a neutral pH by potentiometric or UV-vis measurements at pH 7 (see below), but only at alkaline pH values (see Fig. 7c and d and S14† for H_2L4 and HL2, respectively). The formation of these species can be related to the deprotonation of either metal-coordinated water molecules or of the hydroxyl group of 8-OHQ. However, as discussed above, these ligands are in zwitterionic form at a neutral pH value, the OH group being

deprotonated. This result would suggest that deprotonation at alkaline pH values of the HL2 and H_2L4 complexes involves the hydroxyl group of 8-OHQ, which can also be favored by interactions with the metal, as actually testified by the crystal structure of the $[Pb(HL4)]^+$ cation, in which the metal-bound hydroxyl group is deprotonated.

Receptors L1–H_2L5 as fluorescent probes for metals

To test the ability of the present receptors to optically signal the selected metals, we performed spectrophotometric and spectrofluorimetric titrations in aqueous solutions at 298 K by adding increasing amounts of a metal to a solution of a given receptor at a neutral pH value. The Pb(II) complexes with L1, L3 and H_2L5 suffer from low solubility under these conditions, preventing the analysis of their spectral features. The presence of the metal affects both the absorption and emission spectra of the ligands. Fig. 8 presents, as representative examples of ligands containing Q and 8-OHQ, the absorption spectra of L3 and HL2 in the presence of increasing amounts of Zn(II). The UV-vis spectra of the other systems are given within the ESI (Fig. S18–S22†). Both the quinoline-containing receptors L1 and L3 display the typical structured absorption band of quinoline centred at 305 nm, accompanied by a broad band at *ca.* 270 nm. The addition of Zn(II) to aqueous solutions of L1 or L3 at pH 7 induces the enhancement of the absorbance at 305 nm and a decrease of the 270 nm absorption band. Cd(II) coordination generally induces minor changes in the spectra, while Cu(II) binding leads to a marked enhancement of the absorption band at 270 (see ESI†). The fluorescence emission properties of the receptors are strongly dependent on the coordinated metal ion.

All receptors are basically quenched at a neutral pH value. L1 and L3 at pH 7 are mainly in their diprotonated $[H_2L]^{2+}$ form (L = L1 or L3), with two amine groups of the macrocyclic core being protonated. A previous study on the emission of L1 and L3 found that in their diprotonated form, one (L1) or two (L3) acidic protons are shared *via* H-bonds between the Q nitrogen and the vicinal tertiary amine group of the macrocyclic unit.[23] Considering that Q is a known photo-base,[35] L1 and L3 are probably quenched at pH 7 by a fast excited-state intramolecular proton transfer (ESIPT) process involving the Q nitrogen and the adjacent cyclen amine groups. This process is likely to be inhibited by metal binding, leading to a renewal of the typical fluorescence emission of the Q moiety at 396 nm in the presence of Zn(II), as actually observed in Zn(II) complexation by L1 and, overall, L3 (see Fig. 9). However, a different mechanism involving quenching of the receptor *via a* photoinduced electron transfer (PET) pathway from a not protonated amine group to the fluorophore cannot be completely ruled out. In this case, Zn(II) binding by the cyclen unit would inhibit the PET process, restoring, once again, the Q emission.

As shown in Fig. 9, the L3 emission at 396 nm linearly increases upon Zn(II) addition up to a 1 : 0.8 ligand-to-metal molar ratio. Then the emission intensity still increases more smoothly, to achieve a constant value for a metal-to-ligand molar ratio greater than 1 : 1.2, as expected for the formation of a stable 1 : 1 complex. The emission at 396 nm is *ca.* 4 and 20 times increased in the presence of 1 eq. of Zn(II) in the case of L1 and L3 respectively (Fig. 9b), with quantum yields, Φ, of 0.0065 and 0.022 (Φ = 0.0015 and 0.0016 for L1 and L3 as free ligands, respectively). Limits of detection (LODs) of 9.7 μM and 12 μM were determined for L3 and L1, respectively (Fig. S23†). As normally found in complexes with polyamine-based ligands, Cu(II) complexation does not change the quenched status of the receptors. Similarly, binding of Cd(II) does not remarkably affect the emission of both receptors, probably due to its heavier nature than Zn(II).

However, other factors can affect the emission in metal chelates, including the overall hydrophobic characteristics of the complexes, which can increase their fluorescence emission, strength of the metal–amine bond, which can influence the efficiency of PET process and, finally, thermodynamic stability of the complexes and protonation constants of the polyamine receptor, which determine the percentage of complexes effectively formed at a given pH value. From this point of view, the complexes with L1 and L3 show high stability, sufficient to ensure almost complete metal binding in solutions at a neutral pH value in the presence of a slight excess of metal (1 : 1.2 ligand-to-metal molar ratio). Furthermore, the crystal structure of $[ZnL3]^{2+}$ shows that the two Q units are associated *via* C···C and C···N contacts, giving rise to an overall gathered

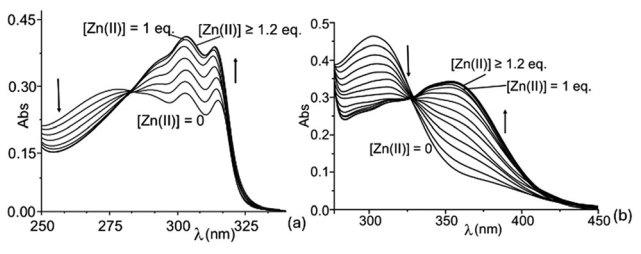

Fig. 8 UV-vis spectra of L3 (a) and HL2 (b) in aqueous solutions at pH 7 in the presence of increasing amounts of Zn(II) ([L3] = 6 × 10^{-6} M, [HL2] = 5.2 × 10^{-5}).

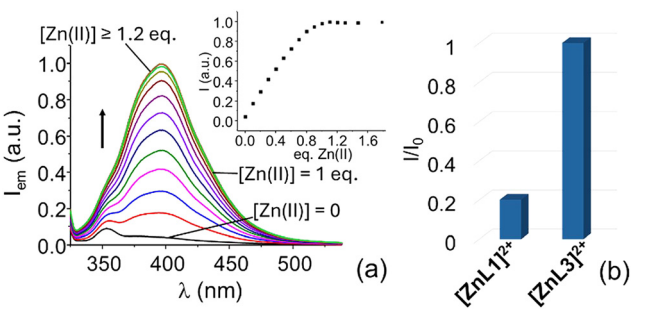

Fig. 9 Emission spectra of L3 in the presence of increasing amounts of Zn(II) (inset: the emission intensity at 396 nm is a function of Zn(II) equivalents added) (a) and comparison of the emission intensity of the Zn(II) complexes with L1 and L3 in the presence of 1 equiv. of Zn(II) (b) ([L1] = [L3] = 1 × 10^{-5} M, λ_{exc} = 316 nm).

and hydrophobic structure that can protect the fluorogenic units, reducing non-radiative deactivation of their excited state, with respect to the $[ZnL1]^{2+}$ complex, which contains a single Q unit. Of note, the crystal structure of the $[CdL3]^{2+}$ complex shows that the two Q moieties are not associated, giving rise to a more 'open' molecular architecture, which would favour the solvation of the fluorogenic units. This could also contribute to the quenching of the fluorescence emission of the complex.

Differently from L1 and L3, Zn(II) complexation by L5 does not increase the emission of the ligand, which is almost not emissive at pH 7. In the [ZnL5] complexes, the metal is likely to be coordinated by the tetraamine framework and by the two carboxylate groups, while the two large hydrophobic Q units are not bound and lie far from the metal cations, as shown by the crystal structure of the $[Ca(ZnL5)_2]^{2+}$ cation. This coordination mode makes the overall structure less gathered, making both Q units more exposed to water molecules, which can therefore contribute to the deactivation of the excited states and consequent emission quenching.

Receptors HL2 and H_2L4 display different sensing properties, due to the presence of one (HL2) or two 8-OHQ (H_2L4) moieties appended to the macrocyclic framework. In fact, the stronger binding ability for metals displayed by 8-OHQ with respect to Q not only increases the stability of the complexes, but also contributes to determine the optical recognition patterns of the fluorescent receptors. Previous studies on the protonation characteristics of HL2 showed that at neutral pH, the receptor is in its $[H_3L2]^{2+}$ protonated form, in which two acidic protons are localized on the tetra-amine macrocyclic unit, while 8-OHQ is in its non-zwitterionic form.[23] The UV-vis absorption spectrum displays a band at *ca.* 300 nm, attributed to the non-zwitterionic form of 8-OH-Q. A second intense band is observed below 250 nm. The addition of Zn(II) or Cd(II) to solutions of HL2 leads to the disappearance of this band and the appearance of a new red-shifted absorption band at *ca.* 355 nm, indicating, as expected, the involvement of 8-OHQ in metal binding (see Fig. 8b and S19†). The latter band cannot be attributed to the deprotonation of the hydroxyl group, which is known to generate a band at a much lower energy (460 nm in 8-OHQ),[23] ruling out the deprotonation of 8-OHQ upon Zn(II) or Cd(II) coordination. The band at 355 nm strongly resembles that observed for the protonated form of 8-OHQ – containing a protonated nitrogen atom – as expected considering that in the HL2 complexes, heteroaromatic nitrogen is bound to a positively charged metal centre, together with the tetra-amine macrocycle. H_2L4, present in solution in its $[H_4L4]^{2+}$ form, shows a similar behaviour, with the formation of a new band at 357 nm in the presence of Zn(II) or Cd(II), confirming that the 8-OHQ units, in non-zwitterionic form, are coordinated to the metal *via* their heteroaromatic nitrogens, as shown by the crystal structures of the $[ZnL4]^{2+}$ and $[CdL4]^{2+}$ complexes. In the case of Cu(II) coordination, the superimposition of the 300 nm band with that at a higher energy makes difficult the interpretation of the spectral changes upon metal coordination (see Fig. S21†).

Differently from the UV-vis absorption characteristics, the fluorescence emission properties of the two receptors in the presence of Zn(II) and Cd(II) markedly differ from one another. In fact, the fluorescence emission of H_2L4 is poorly affected by Zn(II) and Cd(II) binding, while the fluorescence emission of HL2 is enhanced in the presence of Cd(II) (Fig. 10). A slight increase is also observed in the case of Zn(II).

In this case, the interpretation of the emission properties of the two receptors is more intriguing. As observed for L3, the presence of two hydrophobic 8-OHQ units would suggest a higher emission of the H_2L4 complexes with respect to those of HL2. Furthermore, 8-OHQ is a bidentate ligand, whose binding mode results in a stronger interaction with transition and post-transition metals, including Zn(II) and Cd(II), with respect to simple quinoline.

As a matter of fact, the crystal structure of the $[Cd(H_2L4)]^{2+}$ complexes shows that the hydroxyl groups, together with the heteroaromatic nitrogens, of both 8-OHQ moieties are involved in metal binding, leading, as described above, to a displacement of Cd(II) from the mean plane of the macrocyclic ring, greater than that observed for the corresponding complex with L3, and a consequent weakening of the interaction of Cd(II)

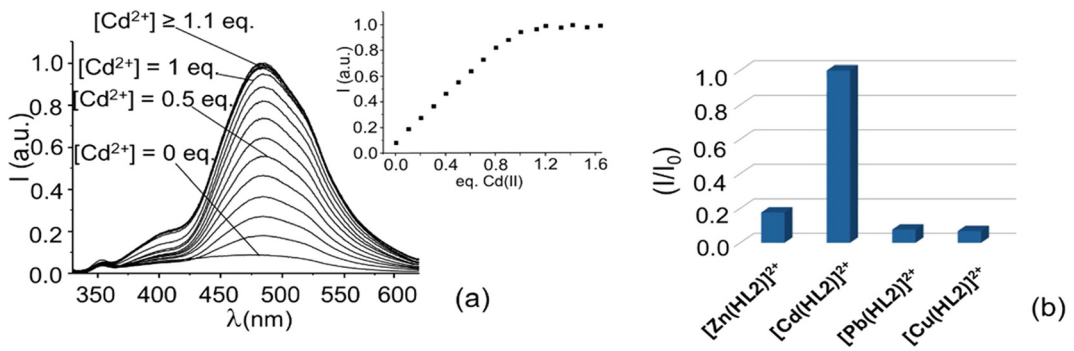

Fig. 10 Emission spectra of HL2 in the presence of increasing amounts of Cd(II) (inset: emission intensity at 484 nm as a function of Cd(II) equivalents added) (a) and comparison of the emission intensity of the complexes with HL2 in the presence of 1 equivalent of Zn(II), Cd(II), Pb(II) and Cu(II) (the I/I_0 values are normalized to the emission of the Cd(II) complex, taken equal to 1) (b) ([HL2] = 9.5×10^{-6} M, λ_{exc} = 320 nm).

with the macrocyclic ring. Strong binding to both 8-OHQ units could also induce detachment of an amine group from the metal in solution. These observations lead us to speculate that the amine groups of the macrocyclic ring could be able to give a PET effect to the 8-OHQ fluorophore, quenching the fluorescence emission of the complex. A similar effect can also be proposed for the $[Zn(H_2L4)]^{2+}$ complex, in which the amine groups of the tetraamine macrocycle are bound at a longer distance than that observed in the emissive Zn(II) complex with L3. Although in this case, the OH groups of 8-OHQ are not bound to the metal, the nitrogen donor of 8-OHQ is a better σ-donor than simple Q, leading to a larger displacement of the metal from the tetra-amine plane.

Conversely, the HL2 complexes with Cd(II), and, at a much lesser extent, Zn(II) displays an emission band at 484, which is attributed to a 8-OHQ unit bound to a positively charged metal centre (Φ = 0.039 and 0.0058 for the Cd(II) and Zn(II) complexes, while Φ = 0.0024 for the 'free' ligand). An LOD value of 10.4 μM was found for Cd(II) detection by HL2. In this case, strong binding of the 8-OHQ moiety to Cd(II) is likely to inhibit any ESIPT process,[34] enhancing the emission of the fluorophore. Furthermore, the presence of a single coordinated metal-bound 8-OHQ unit in HL2 can reduce the displacement of the metal from the macrocyclic plane, observed for the $[Cd(H_2L4)]^{2+}$ complex, reinforcing its interaction with the aliphatic amine groups of the macrocycle, thus inhibiting a possible quenching PET effect from the aliphatic amine groups. The lower emission intensity observed in the case of Zn(II) could imply a dynamic equilibrium involving 8-OHQ detachment from the metal, enabling, once again, an ESIPT[35] process able to reduce the emission.

The recognition ability of L1–H_2L5 was finally tested by recording the emission spectra of the ligands (Fig. 11) in the presence of 1 eq. of different metals including Na(I), K(I), Mg(II), Ca(II), Hg(II), Fe(II), Co(II) Mn(II) and Hg(II). The results resumed in Fig. 11 indicate, once again, selective signalling of Zn(II) by L1 and, overall, L3, and of Cd(II) by HL2.

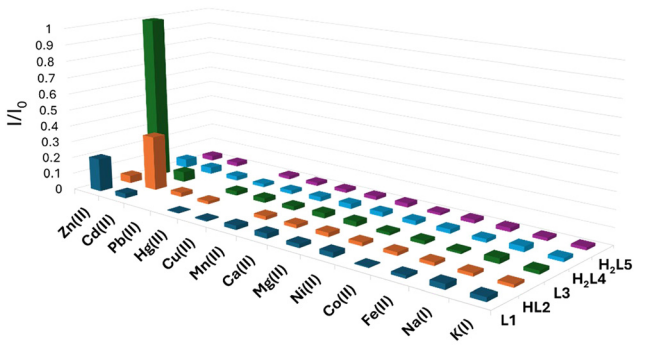

Fig. 11 Emission intensity of L1, L3 and H_2L5 at 396 nm and of HL2 and H_2L4 at 486 nm in the presence of 1 equivalent of different metal cations (aqueous solution at pH 7, TRIS buffer, 298 K; the I/I_0 values are normalized to the emission of the Zn(II) complex with L3, taken equal to 1).

Experimental section

Receptors L1, HL2, L3 and H_2L5 were synthesized as previously described.[23,36] H_2L4 has been synthesized by using a similar procedure to that reported for L3,[36] which exploits the bisaminal method, using, as the starting material, the bis-aminal derivative of the tetraamine macrocycle 1,4,7,10-tetraazacyclododecane (cyclen), *i.e.*, decahydro-2a,4a,6a,8a-tetraaza-cyclopenta[*fg*]acenaphthylene.[36] The crystals of the complexes suitable for X-ray analysis were generally obtained by slow evaporation of the aqueous solution of the receptors (0.001 M) in the presence of 1 equiv. of metal as a perchlorate salt, adjusting the pH value of the solution at 7. Full details for the synthesis of H_2L4 and of the metal complexes are reported in the ESI.†

X-ray crystallography

Single-crystal diffraction measurement for compounds $[CuL1](ClO_4)_2{\cdot}0.5H_2O$, $[ZnL3](ClO_4)_2{\cdot}0.5H_2O$, $[CdL3](ClO_4)_2{\cdot}H_2O$, $[Cd(H_2L4)](ClO_4)_2{\cdot}H_2O$, $[Pb(HL4)]ClO_4{\cdot}(H_2O)_2$, $[Zn(H_2L4)](ClO_4)_2{\cdot}H_2O$ and $[Ca(ZnL5)_2](ClO_4)_2{\cdot}14H_2O$ was carried out using an Oxford Diffraction Excalibur diffractometer with Mo-K_α radiation (λ = 0.71073 Å) and Cu-K_α radiation ($[CuL1](ClO_4)_2{\cdot}H_2O$ – λ = 1.54184 Å). Data collection were performed with the program CrysAlis CCD.[37] Data reductions were carried out with the program CrysAlis RED.[37] Finally, absorption correction was performed with the program ABSPACK in CrysAlis RED.[37]

The structures were solved using the SIR-2004 package[38] and refined by full-matrix least squares against F^2 with all data using SHELXL-2018/3[39] and SHELXL-2014/7 ($[CuL1](ClO_4)_2{\cdot}0.5H_2O$).[40] A summary of the Crystallographic data and refinement parameters is given in Tables S7 and S8.†

$[CuL1](ClO_4)_2{\cdot}0.5H_2O$. All non-hydrogen atoms were anisotropically refined, and all hydrogen atoms were introduced at calculated positions and refined by using a riding model. Perchlorate anions are affected by disorder and each one has been found to spread over two equally populated positions.

$[ZnL3](ClO_4)_2{\cdot}0.5H_2O$. All the ligand non-hydrogen atoms were anisotropically refined. The hydrogen atoms of the ligand were found in the Fourier density map, and their coordination was freely refined, while their thermal parameter was set in accordance to that of the atom to which they are bonded. One of the two perchlorate anions was affected by disorder that was refined by using three models for each oxygen atoms (occupancy factors: 0.48704, 0.25380 and 0.25961, respectively), oxygen atoms were isotropically refined (while those of the other perchlorate anion were anisotropically refined). The water molecule has an occupancy factor of 0.5, its oxygen atom was isotropically refined, while the hydrogen atoms were not introduced in the refinement.

$[CdL3](ClO_4)_2{\cdot}H_2O$. All the non-hydrogen atoms, with the exception of the oxygen ones belonging to the disordered perchlorate anion (see below), were anisotropically refined. The hydrogen atoms of the ligand were set in a calculated position, while those belonging to the water molecule were found in the Fourier density map; their coordination was freely refined,

while their thermal parameter was set in accordance to the water oxygen atom. One of the two perchlorate anions was affected by disorder that was refined by using three models for each oxygen atoms (occupancy factors: 0.40410, 0.32971 and 0.26697). Its oxygen atoms were isotropically refined.

$[Cd(H_2L4)](ClO_4)_2\cdot H_2O$. All the non-hydrogen atoms were anisotropically refined. The hydrogen atoms of the water molecules, as well as those bonded to O1 and O2, were found in the Fourier density map, and their coordination was freely refined while their thermal parameter was set in accordance with that of the atom to which they are bonded. All the other hydrogen atoms of the ligand were set in calculated position.

$[Pb(HL4)]ClO_4\cdot(H_2O)_2$. All the non-hydrogen atoms were anisotropically refined. The hydrogen atoms of the water molecule, as well as those bonded to N1, N3 and O1 were found in the Fourier density map, and their coordination was freely refined while their thermal parameter was set in accordance with that of the atom to which they are bonded. All the other hydrogen atoms of the ligand were set in the calculated position.

$[Zn(H_2L4)](ClO_4)_2\cdot H_2O$. All the non-hydrogen atoms were anisotropically refined. The hydrogen atoms of the water molecule, as well as those bonded to O1 and O2, were found in the Fourier density map, their coordination was freely refined, while their thermal parameter was set in accordance with that of the atom to which they are bonded. All the other hydrogen atoms of the ligand were set in the calculated position.

$[Ca(ZnL5)_2](ClO_4)_2\cdot 14H_2O$. All non-hydrogen atoms, with the exception of those belonging to the disordered perchlorate anion and water molecule (see below), were anisotropically refined; the hydrogen atoms of the ligand were set in the calculated position, while those atoms of the water molecules (with the exception of the disordered one) were found in the Fourier density map, and their coordination was freely refined, while their thermal parameter was set in accordance to the water oxygen atom. One of the two perchlorate anions was affected by disorder that was refined by using two models for each oxygen atom (occupancy factors: 0.6 and 0.4), these atoms were isotropically refined. Finally, for the disordered water molecule, two models for the oxygen atoms were used (occupancy factors: 0.5 and 0.5) and the hydrogen atoms of this water molecule were not introduced in the refinement.

Potentiometric measurements

All pH measurements ($pH = -\log[H^+]$) employed for the determination of the constants for complex formation were carried out in a 0.1 M NaCl aqueous solution at 298.0 ± 0.1 K by means of conventional titration experiments in an inert atmosphere. The used equipment and procedures have previously been described.[41] The standard potential E° and the ionic product of water were determined by Gran's method.[42] At least three measurements (with about 100 data points for each) were performed for each system. In all experiments, the ligand concentration [L] was about 1×10^{-3} M, while the metal concentration was varied from 0.5×10^{-3} M to 1.8×10^{-3} M. The computer program HYPERQUAD[43] was used to calculate the equilibrium constants from the emf data.

UV-vis and fluorescence emission spectroscopies

Absorption and fluorescence spectra were recorded using a PerkinElmer Lambda 6 spectrophotometer and a PerkinElmer LS55 spectrofluorimeter or Horiba FluoroMax Plus instruments, respectively, by using cuvettes with 10 mm optical path length. In the spectrophotometric/spectrofluorimetric titrations, a 0.1 M aqueous solution of the metals was added to a 1×10^{-5} M aqueous solution of the receptors, buffered at pH 7 with TRIS 0.01 M. The pH was measured with a glass electrode. All measurements were performed at 298.0 ± 0.1 K.

The detection limits (LODs) for Zn(II) by **L1** and **L3** and for Cd(II) by **HL2** were determined by using a reported method.[44,45] Fluorescence titrations were performed by adding increasing amounts of the metal to receptors and measuring the fluorescence emission. The fluorescence spectrum of the probes in the absence of metal cations (blank) at pH 7.0 in TRIS buffer was measured ten times, achieving the standard deviation, σ_b, calculated on the emission maximum of the blank. A linear relationship between the fluorescence emission of probes and metal ion concentration was obtained in the ranges of 1–3 μM (L1) and 1–5 μM (HL2 and L3) (Fig. S23†). The LOD was calculated by using the equation: $LOD = 3\sigma_b/K$, where K is the slope of the line obtained by plotting the emission intensity *vs.* metal concentration.

The luminescence quantum yields were determined using quinine sulfate in a 0.05 M H_2SO_4 aqueous solution ($\Phi = 0.53$) as a standard reference.[46]

Concluding remarks

This study used a series of receptors composed of a common tetraamine macrocycle, cyclen, with simple and largely used quinoline and 8-hydroxyquinoline, to demonstrate that the optical recognition of Zn(II) and Cd(II), two transition metals with similar electronic characteristics, is ruled not only by the thermodynamic stability of complexes, but also by the subtle structural motifs that, in turn, manage the deactivation patterns of the excited fluorophore *via* proton transfer processes and fluorophore solvation. Among the five receptors, the Q-containing receptor L3, and to a much lesser extent, L1, can optically discriminate Zn(II) over Cd(II), while the 8-OH-Q-based HL2 receptor can selectively recognize Cd(II) over Zn(II). This different ability cannot be related to the different binding affinity of the receptors for the two metals (for instance, Zn(II) forms somewhat less stable complexes with L3 with respect to H_2L4), but can be related to the structural characteristics of the complexes. The emissive $[ZnL3]^{2+}$ complex is featured by two associated fluorogenic units and by a gathered and hydrophobic structure, which may reduce the contacts of the Q units with water molecules. In the corresponding Cd(II) complex, the two Q units are poorly associated, leading to a more open structure, which favours solvation of the fluorogenic units.

Larger fluorophore solvation, together with the heavier nature of Cd(II), can deactivate the excitation state of the cadmium complex *via* a non-radiative pattern. A different scenario is depicted by the complexes with HL2 and H_2L4, whose 8-OHQ moieties feature a much better binding ability than Q. In the H_2L4 complexes with Zn(II) or Cd(II), the binding of 8-OHQ to the metals induces their displacement from the macrocyclic plane, weakening their interactions with the cyclen amine groups, which, in turn, may quench the fluorophore emission *via* a PET process. In the case of complexes with HL2, only a single 8-OHQ moiety is bound to the metal, probably inducing a minor detachment from the cyclen plane in the case of the larger Cd(II) ion, justifying the emissive state of the complex.

Author contributions

G. M. R., Y. T. S. S., F. B. and L. C. performed the synthetic work and the solution study; E. M., C. B., P. R. and P. P. collected the structure and solved the X-ray structures; M. I., G. M. R., A. B. and M. S. designed the study; A. B. and M. S. supervised the study and written the paper.

Data availability

Crystallographic data for and $[CuL1](ClO_4)_2{\cdot}0.5H_2O$, $[Zn(H_2L4)](ClO_4)_2{\cdot}H_2O$, $[Pb(HL4)]ClO_4{\cdot}(H_2O)_2$, $[CdL3](ClO_4)_2{\cdot}H_2O$, $[ZnL3](ClO_4)_2{\cdot}0.5H_2O$, $[Cd(H_2L4)](ClO_4)_2{\cdot}H_2O$, and $[Ca(ZnL5)_2](ClO_4)_2{\cdot}14H_2O$ have been deposited at the CCDC with deposition number 2375275, 2375276, 2375277, 2375278, 2375279, 2375280 and 2375281, respectively. Other experimental data that support the results of this study are available in the main article or in the ESI.†

Conflicts of interest

There are no conflicts to declare.

Acknowledgements

G. M. R., M. I. and A. B acknowledge Regione Toscana for financial support of the MetalRec Project within the program 'Progetti di alta formazione attraverso l'attivazione di assegni di ricerca' nell'ambito della transizione verde.

References

1 (*a*) K. Raeissi, A. Saatchi, M. A. Golozar and J. A. Szpunar, *J. Appl. Electrochem.*, 2004, **34**, 1249–1258; (*b*) A. Khansole, S. Basak, T. K. Pal and M. Shome, *Int. J. Mater. Res.*, 2023, **114**, 425–430.

2 (*a*) M. Tribbia, G. Zampardi and F. La Mantia, *Curr. Opin. Electrochem.*, 2023, **28**, 101230; (*b*) L. Zhenjie and X. Murong, *J. Electrochem. Soc.*, 2022, **169**, 120508; (*c*) S. D. Pu, C. Gong, Y. T. Tang, Z. Ning, J. Liu, S. Zhang, Y. Yuan, D. Melvin, S. Yang, L. Pi, J.-J. Marie, B. Hu, M. Jenkins, Z. Li, B. Liu, S. C. E. Tsang, T. J. Marrow, R. C. Reed, X. Gao, P. G. Bruce and A. W. Robertson, *Adv. Mater.*, 2022, **34**, 2202552.

3 (*a*) Y. Li, L. Wen and W. Guo, *Chem. Soc. Rev.*, 2023, **52**, 1168–1188; (*b*) C. Rousseau, F. Baraud, L. Leleyter and O. Gil, Cathodic protection by zinc sacrificial anodes: Impact on marine sediment metallic contamination, *J. Hazard. Mater.*, 2009, **167**, 953–958.

4 (*a*) L. A. Roudabush, *J. Mater. Manuf.*, 1990, **99**, 720–728; (*b*) F. E. Goodwin, in *Kirk-Othmer Encyclopedia of Chemical Technology*, Wiley & Sons Ed., 2012, pp. 789–839.

5 I. Bertini, H. B. Gray, E. I. Stiefel and V. J. Selverstone, *Biological Inorganic Chemistry: Structure and Reactivity*, University Science Books, Sausalito, California, 2007.

6 (*a*) J. Olechnowicz, A. Tinkov, A. Skalny and J. Suliburska, *J. Physiol. Sci.*, 2018, **68**, 19–31; (*b*) L. I. Stiles, K. Ferrao and K. J. Mehta, *Clin. Exp. Med.*, 2024, **24**, 38.

7 S. Mashhadikhan, A. E. Amooghin, H. Sanaeepur and M. M. A. Shirazi, *Desalination*, 2022, **535**, 115815.

8 G. Genchi, M. S. Sinicropi, G. Lauria, A. Carocci and A. Catalano, *Int. J. Environ. Res. Public Health*, 2020, **17**, 3782.

9 C. Ballabio, A. Jones and P. Panagos, *Sci. Total Environ.*, 2024, **912**, 168710.

10 (*a*) X. Liu, N. Zhang, J. Zhou, T. Chang, C. Fang and D. Shangguan, *Analyst*, 2013, **138**, 901–906; (*b*) D. Zhang, S. Li, R. Lu, G. Liu and S. Pu, *Dyes Pigm.*, 2017, **146**, 305–315; (*c*) L. Xue, C. Liu and J. Hua, *Org. Lett.*, 2009, **11**, 1655–1658; (*d*) J. Li, Y. Chen, T. Chen, J. Qiang, Z. Zhang, T. Wei, W. Zhang, F. Wang and X. Chen, *Sens. Actuators, B*, 2018, **268**, 446–455; (*e*) A. Garau, M. C. Aragoni, M. Arca, A. Bencini, A. J. Blake, C. Caltagirone, C. Giorgi, V. Lippolis and M. A. Scorciapino, *ChemPlusChem*, 2020, **85**, 1789–1799; (*f*) M. C. Aragoni, M. Arca, A. Bencini, C. Caltagirone, A. Garau, F. Isaia, M. E. Light, V. Lippolis, C. Lodeiro, M. Mameli, R. Montis, M. C. Mostallino, A. Pintus and S. Puccioni, *Dalton Trans.*, 2013, **42**, 14516–14530; (*g*) M. Formica, G. Ambrosi, V. Fusi, L. Giorgi, M. Arca, A. Garau, A. Pintus and V. Lippolis, *New J. Chem.*, 2018, **42**, 7869–7883.

11 B. Valeur, *Molecular fluorescence principles and applications*, Wiley-VCH, Weinheim, 2001.

12 (*a*) D. Wu, A. C. Sedgwick, T. Gunnlaugsson, E. U. Akkaya, J. Yoon and T. D. James, *Chem. Soc. Rev.*, 2017, **46**, 7105–7123; (*b*) V. Amendola, M. Bonizzoni, D. Esteban-Gómez, L. Fabbrizzi, M. Licchelli, F. Sancenón and A. Taglietti, *Coord. Chem. Rev.*, 2006, **250**, 1451–1470; (*c*) V. Balzani, G. Bergamini and P. Ceroni, *Coord. Chem. Rev.*, 2008, **252**, 2456–2469; (*d*) B. Valeur and I. Leray, *Coord. Chem. Rev.*, 2000, **205**, 3–40; (*e*) A. Bianchi, E. Delgado-Pinar, E. Garcia-España, C. Giorgi and F. Pina, *Coord. Chem. Rev.*, 2014, **260**, 156–215.

13 (*a*) M. Formica, V. Fusi, L. Giorgi and M. Micheloni, *Coord. Chem. Rev.*, 2012, **256**, 170–192; (*b*) C. Lodeiro,

J. L. Capelo, J. C. Mejuto, E. Oliveira, H. M. Santos, B. Pedras and C. Nuñez, *Chem. Soc. Rev.*, 2010, **39**, 2948–2976; (*c*) B. Kaur, N. Kaur and S. Kumar, *Coord. Chem. Rev.*, 2018, **358**, 13–69.

14 (*a*) C. Caltagirone and P. A. Gale, *Chem. Soc. Rev.*, 2009, **38**, 520–563; (*b*) Y. Ding, W.-H. Zhu and Y. Xie, *Chem. Rev.*, 2017, **117**, 2203–2256; (*c*) J. A. Cotruvo Jr, A. T. Aron, K. M. Ramos-Torres, M. Karla and C. J. Chang, *Chem. Soc. Rev.*, 2015, **44**, 4400–4414.

15 (*a*) X. Qian and Z. Xu, *Chem. Soc. Rev.*, 2015, **44**, 4487–4493; (*b*) C. Lodeiro and F. Pina, *Coord. Chem. Rev.*, 2009, **253**, 1353–1383; T. Joshi, B. Graham and L. Spiccia, *Acc. Chem. Res.*, 2015, **48**, 2366–2379.

16 (*a*) V. Amendola, L. Fabbrizzi, F. Foti, M. Licchelli, C. Mangano, P. Pallavicini, A. Poggi, D. Sacchi and A. Taglietti, *Coord. Chem. Rev.*, 2006, **250**, 273–299; (*b*) L. Prodi, F. Bolletta, M. Montalti and N. Zaccheroni, *Coord. Chem. Rev.*, 2000, **205**, 59–83; (*c*) R. Martínez-Máñez and F. Sancenón, *Chem. Rev.*, 2003, **103**, 4419–4476; (*d*) N. Busschaert, C. Caltagirone, W. Van Rossom and P. A. Gale, *Chem. Rev.*, 2015, **115**, 8038–8155.

17 (*a*) K. P. Carter, A. M. Young and A. E. Palmer, *Chem. Rev.*, 2014, **114**(8), 4564–4601; (*b*) S. Shinoda, *Chem. Soc. Rev.*, 2013, **42**, 1825; (*c*) H. Zhu, J. Fan, B. Wang and X. Peng, *Chem. Soc. Rev.*, 2015, **44**, 4337–4366.

18 (*a*) C.-T. Shi, Z.-Y. Huang, A.-B. Wu, Y.-X. Hu, N.-C. Wang, Y. Zhang, W.-M. Shu and W.-C. Yu, *RSC Adv.*, 2021, **11**, 29632; (*b*) S.-Y. Chen, Z. Li, K. Li and X.-Q. Yu, *Coord. Chem. Rev.*, 2021, **429**, 213691.

19 S. Nazerdeylami, J. B. Ghasemi, A. Amiri, G. M. Ziarani and A. Badiei, *Methods Appl. Fluoresc.*, 2020, **8**, 025009.

20 (*a*) P. Wang, L. P. Duan and Y. W. Liao, *Microchem. J.*, 2019, **146**, 818–827; (*b*) P. Wang, K. Chen and Y. S. Ge, *J. Lumin.*, 2019, **208**, 495–501; (*c*) P. Wang, D. G. Zhou and B. Chen, *Spectrochim. Acta, Part A*, 2019, **207**, 276–283; (*d*) P. Wang, Y. An and Y. W. Liao, *Spectrochim. Acta, Part A*, 2019, **216**, 61–68; (*e*) P. Wang, J. Wu and C. H. Zhao, *Spectrochim. Acta, Part A*, 2020, **226**, 117600.

21 J. K. Xiong, K. R. Wang, K. X. Wang, T. L. Han, H. Y. Zhu, R. X. Rong, Z. R. Cao and X. L. Li, *Sens. Actuators, B*, 2019, **297**, 126802.

22 W. B. Huang, W. Gu, H. X. Huang, J. B. Wang, W. X. Shen, Y. Y. Lv and J. Shen, *Dyes Pigm.*, 2017, **143**, 427–435.

23 F. Bartoli, L. Conti, G. M. Romano, L. Massai, P. Paoli, P. Rossi, G. Pietraperzia, C. Gellini and A. Bencini, *New J. Chem.*, 2021, **45**, 16926–16938.

24 S. Aoki and E. Kimura, *Chem. Rev.*, 2004, **104**, 769.

25 (*a*) T. Koike, T. Watanabe, S. Aoki, E. Kimura and M. Shiro, *J. Am. Chem. Soc.*, 1996, **118**, 12696; (*b*) S. Aoki, S. Kaido, H. Fujioka and E. Kimura, *Inorg. Chem.*, 2003, **42**, 1023; (*c*) R. Ohshima, M. Kitamura, A. Morita, M. Shiro, Y. Yamada, M. Ikekita, E. Kimura and S. Aoki, *Inorg. Chem.*, 2010, **49**, 888; (*d*) M. Kitamura, T. Suzuki, R. Abe, T. Ueno and S. Aoki, *Inorg. Chem.*, 2011, **50**, 11568.

26 I.-T. Lim and K.-Y. Choi, *Main Group Met. Chem.*, 2011, **34**, 5–6.

27 (*a*) N. B. Sankaran, P. K. Mandal, B. Bhattacharya and A. Samanta, *J. Mater. Chem.*, 2005, **15**, 2854–2859; (*b*) Y. Shiraishi, Y. Kohno and T. Hirai, *J. Phys. Chem. B*, 2005, **109**(41), 19139–19147; (*c*) B. B. Correia, T. R. Brown, J. H. Reibenspies, H. S. Lee and R. D. Hancock, *Eur. J. Inorg. Chem.*, 2018, **33**, 3736–3747; (*d*) M. Li, L. Meng, H.-Y. Lu, R.-L. Liu, J.-D. Chen and C.-F. Chen, *J. Org. Chem.*, 2012, **77**, 3670–3673.

28 R. M. Smith and A. E. Martell, *NIST Critically Selected Stability Constants of Metal Complexes Database (NIST Standard Reference Database 46), version 8.0*, National Institute of Science and Technology, Gaithersburg, MD, 2004.

29 R. Nasanen and U. Penttinen, *Acta Chem. Scand.*, 1952, **6**, 837–843.

30 A. Garau, G. Picci, A. Bencini, C. Caltagirone, L. Conti, V. Lippolis, P. Paoli, G. M. Romano, P. Rossi and M. A. Scorciapino, *Dalton Trans.*, 2022, **51**, 8733–8742.

31 J. Dale, *Acta Chem. Scand.*, 1973, **27**, 1115–1129.

32 A. W. Addison, T. N. Rao, J. Reedijk, J. van Rijn and G. C. Verschoor, *J. Chem. Soc., Dalton Trans.*, 1984, 1349–1356.

33 (*a*) R. D. Hancock, M. Salim Shaikjee, S. M. Dobson and J. C. A. Boeyens, *Inorg. Chim. Acta*, 1988, **154**, 229–238; (*b*) C. Bazzicalupi, A. Bencini, S. Biagini, A. Bianchi, E. Faggi, C. Giorgi, M. Marchetta, F. Totti and B. Valtancoli, *Chem. – Eur. J.*, 2009, **15**, 8049–8063; (*c*) A. Andrés, A. Bencini, A. Carachalios, A. Bianchi, P. Dapporto, E. García-España, P. Paoletti and P. Paoli, *J. Chem. Soc., Dalton Trans.*, 1993, 3507–3513.

34 The mean distance between Zn(II) and aliphatic amine groups have been found *via* a search on the Cambridge Structural Database: C. R. Groom, I. J. Bruno, M. P. Lightfoot and S. C. Ward, *Acta Crystallogr., Sect. B: Struct. Sci., Cryst. Eng. Mater.*, 2016, **72**, 171–179.

35 E. W. Driscoll, J. R. Hunt and J. M. Dawlaty, *J. Phys. Chem. Lett.*, 2016, **7**, 2093–2099; S.-Y. Park, P. Ghosh, S. O. Park, Y. M. Lee, S. K. Kwak and O.-H. Kwon, *RSC Adv.*, 2016, **6**, 9812–9821.

36 M. Becatti, A. Bencini, S. Nistri, L. Conti, M. G. Fabbrini, L. Lucarini, V. Ghini, M. Severi, C. Fiorillo, C. Giorgi, L. Sorace, B. Valtancoli and D. Bani, *Sci. Rep.*, 2019, **9**, 10320.

37 *CrysAlisPro*, Agilent Technologies, 2011.

38 M. C. Burla, R. Caliandro, M. Camalli, B. Carrozzini, G. L. Cascarano, L. Da Caro, C. Giacovazzo, G. Polidori and R. Spagna, *J. Appl. Crystallogr.*, 2005, **38**, 381–388.

39 G. M. Sheldrick, *Acta Crystallogr., Sect. C:Struct. Chem.*, 2015, **71**, 3–8.

40 G. M. Sheldrick, *SHELXL-2014/1, Program for Crystal Structure Refinement*, University of Göttingen, Göttingen, 2014.

41 C. Bazzicalupi, A. Bencini, S. Biagini, E. Faggi, S. Meini, C. Giorgi, A. Spepi and B. Valtancoli, *J. Org. Chem.*, 2009, **74**, 7349–7363.

42 G. Gran, *Analyst*, 1952, **77**, 661–671.

43 P. Gans, A. Sabatini and A. Vacca, *Talanta*, 1996, **43**, 1739–1753.
44 Y. Sun, Y. Liu and W. Guo, *Sens. Actuators, B*, 2009, **143**(1), 171–176.
45 Q. Mei, Y. Shi, Q. Hua and B. Tong, *RSC Adv.*, 2015, **5**, 74924–74931.
46 M. J. Adams, J. G. Highfield and G. F. Kirkbright, *Anal. Chem.*, 1977, **49**, 1850–1852.